S. Lakshmi Tulasi[*1] , P. Sumalatha [2] , N. Usha Rani[1], Pavani Peddi[1]

[1]*PVP Siddhartha Institute of Technology, Kanuru, Vijayawada, Andhra Pradesh, India;*
[2]*Seshadri Rao Gudlavalleru Engineering college, Gudlavalleru. Andhra Pradesh, India*
(*Corresponding author's e-mail: tulasi13111986@gmail.com)

Green Synthesis, Characterization and Environmental Application of Copper Oxide Nanoparticle obtained Using Aqueous Extract of *Schrebera Swietenioides Roxb.*

The goal of the present study was to synthesize the nanoparticles using green methodology with the use of the aqueous plant extract of *S. swietenioides*. The copper oxide nanoparticle has been synthesized using aqueous root extract of *S. swietenioides* as a green reducing agent and copper sulfate as source of the metal ions. Formation of the nanoparticles in the reaction mixture was preliminary confirmed by the UV-Vis spectroscopy method. The FT-IR analysis of the synthesized nanoparticles shows the involvement of various bioactive functional groups in the formation of nanoparticles. The UV–Vis absorption spectra indicate the characteristic maximum absorption peak at a wavelength of 340 nm. This confirms the formation of nano-sized copper particles. The SEM analysis of the synthesized copper oxide nanoparticles confirms that the particles have mostly spherical shape with rough surfaces and the size of 21-43 nm. The copper nanoparticles in the media of the aqueous root extract of *S swietenioides* have been studied for their applications in the photo catalytic reduction of pollutant dyes and metals. The synthesized nanoparticles have been characterized and it was proved that the particles were nano-sized and contained high metal percentage.

Keywords: green synthesis, plant extract, *S. Swietenioides*, copper oxide nanoparticle, UV–visible spectrophotometer, FT-IR, SEM, Photo catalytic activity.

Introduction

Plants are considered as cost-efficient and eco-friendly chemical reagents. Plants act as potential heavy metal detoxificants and are being to overcome the problems caused by various environmental pollutants. These pollutants are very toxic even at the trace levels [1]. The synthesis of NPs using plant extracts considered as clean and environmentally accepted "green chemistry" concept [2].

The synthesis of NPs using plant extracts has considerable advantage on the synthesis with the use of microorganisms due to the complex preservation process of the microbial strains as well as contamination-free maintenance of the culture [3]. The kinetics of the NPs synthesis using plant extracts was higher than in the other green synthesis approaches and equal to the NPs synthesis using chemical methods. The different parts of the plant such as seeds, fruits, leaves, stem, bark, roots etc., are widely used in the synthesis of NPs due to the excellent phytochemicals they produce [4]. A wide range of metal NPs, such as silver, gold, iron, zinc, copper etc. have been synthesized using green approach.

Plant extracts are widely used in the synthesis of CuO NPs nowadays. The synthesis of CuO NPs using plant extracts involves simple, convenient and easy procedure with low energy consumption that produces more stable NPs. During the synthesis of CuO NPs by green methodology, cupric acetate, copper chloride dihydrate, and copper sulphate pentahydrate were generally used as metal ions source [5]. In the process of synthesis and storage of copper NPs, copper tends to oxidize easily and hence stabilizing or capping agent is needed for preventing oxidation and agglomeration. Various properties of NPs such as light absorption, surface morphology, size, shape, crystalline nature etc., were characterized using various techniques. The diverse properties of the NPs were greatly influenced by their shape which was determined by the microscopy techniques. The morphology, surface information and dispersion of the NPs were determined with scanning electron microscope (SEM). Formation of the nanoparticles in the reaction mixture was preliminary confirmed by the UV-Vis spectroscopy method. The UV-vis absorption spectra shows the characteristic maximum absorption peak at a wavelength of 379 nm, which confirms that the nanoparticles are mono-dispersed and narrow in size. The copper and CuO NPs are multifunctional in nature and hence are having wide range

of applications in varies field. The photo catalytic activity of the copper nanoparticles in the media of the aqueous root extract of *S swietenioides* were determined using different pollutant, carcinogenic dyes and heavy metals. The copper nanoparticles in the media of the aqueous root extract of *S swietenioides* were studied for their photo catalytic degradation efficiency on pollutant dyes (sudan red (III) and azure A) and pollutant metal lead. These NPs were applied as antimicrobial agents, photo catalytic agent for degradation of pollutants, anticarcinogenic agent and were used in the formation of biofilms [6, 7]. These NPs can be successfully applied for the improvement of agriculture [8, 9] and food packaging.

Experimental

Chemicals and reagents:

The chemicals used in the study such as copper sulphate pentahydrate, sodium hydroxide, hydrogen peroxide, dibasic disodium phosphate, monobasic sodium di-hydrogen phosphate, sudan red dye, azure A dye, lead nitrate were of analytical reagent grade and were purchased from Merck chemicals and SD fisher scientific, Mumbai.

Collection of plant material:

The roots of the plant *Schrebera swietenioides* Roxb., were collected in the hill area located in Tirumala, Tirupati, Andhra Pradesh. The collected plant sample was authenticated by Dr.Ch. Srinivasa Reddy, Assistant Professor, Department of Botany, SRR & CVR Government Degree College (A) Vijayawada with plant authentication number SRR-CVR/ 2019-20/Bot/31. The collected roots surface was cleaned using sterile cotton and distilled water in order to remove the sand and dirt. Then the water particles on the cleaned material were removed using tissue paper and the plant material was cut onto the small pieces, which were dried up under the shade and preserved.

Extractions of plant materials:

An accurately weighed 10 grams of plant powder was put in a 250 mL beaker containing 100 mL of double distilled water. The plant material with water was boiled on a hot plate at 40 °C for 80 min. The phytochemical constituents present in the plant material were extracted to the water solvent. Then the extract was filtered, the plant material obtained as sediment was discarded and the clear filtrate was made up to 100 mL with distilled water. The clear filtrate obtained was used for the synthesis of nanoparticles [10].

Root Extract Mediated Copper oxide Nanoparticles:

The synthesis of copper oxide nanoparticles using aqueous root extract of *S swietenioides* was carried based on the methodology [11] with minor modifications. After the addition of the 400 mL of 5 mM copper sulphate and 50 mL of aqueous root extract into the 500 mL volumetric flask, the pH of the solution was adjusted to 7 with the 1N sodium hydroxide solution. The change in the colour of the reaction mixture and the formation of particles was observed as an indication of the formation of copper nanoparticles. Then it was centrifuged, supernatant was discarded and precipitate was collected carefully. Residual plant extract was removed by washing the precipitate with excess distilled water. The purified precipitate was collected and dried at 60 °C for 2 h in a hot air oven. Dark brown colour copper nanoparticles were obtained and characterized (Fig. 1).
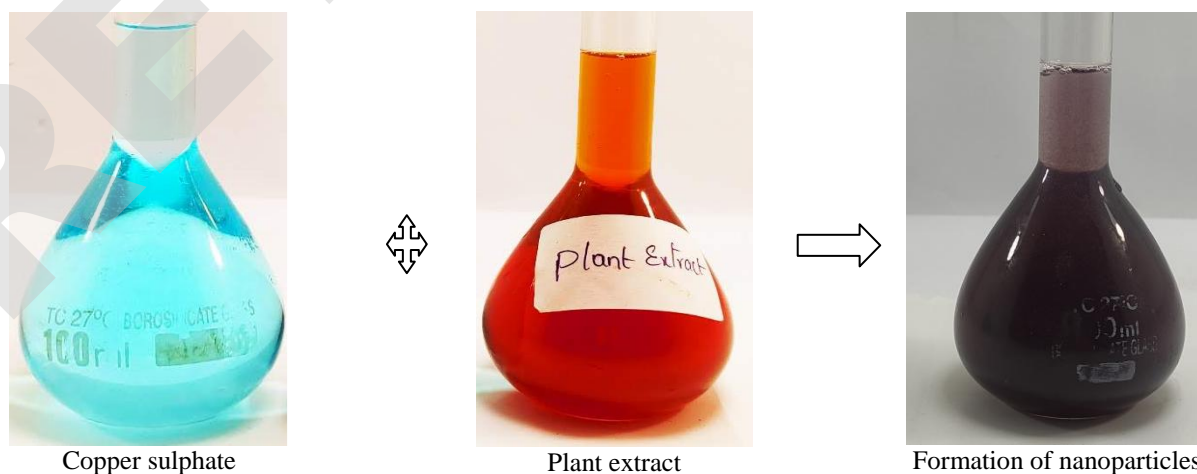

| Copper sulphate | Plant extract | Formation of nanoparticles |

Figure 1. Colour changing observed during the synthesis of copper oxide nanoparticles

Characterization of nanoparticles:

The synthesized copper nanoparticles were characterized using various characterization techniques such as UV-vis spectroscopy (JASCO spectrometer, Japan), FT-IR(Bruker, USA), SEM (NOVA NANOSEM450, FEI USA), XRD(Rigaku Corporation, Japan). The size, shape, surface morphology, functional groups and chemical composition of the copper nanoparticles in the media of the aqueous root extract of *S swietenioides* were also determined [12, 13].

Photo catalytic activity of nanoparticles:

The photo catalytic activity of the copper nanoparticles in the media of the aqueous root extract of *S swietenioides* were determined using different pollutant, carcinogenic dyes and heavy metals. Copper nanoparticles in the media of the aqueous root extract of *S swietenioides* were studied for their photo catalytic degradation efficiency on pollutant dyes (sudan red (III) and azure A) and pollutant metal lead [14–16].

UV-visible spectrophotometer:

The UV-vis spectroscopy analysis of the colour change observed during the addition of aqueous root extract of *S. swietenioides* and copper metal solution was carried out. The UV–Vis absorption spectra shows the characteristic maximum absorption peak at a wavelength of 340 nm. This confirms the formation of nano-sized copper particles [17]. The similar type of absorption peak was not identified in the absorption spectra of plant root extract as well as the aqueous copper metal solution. Hence it can be confirmed the characteristic wavelength maximum is due to the formation of copper oxide nanoparticles. Figure 2 shows the absorption spectra of synthesized copper oxide nanoparticles.
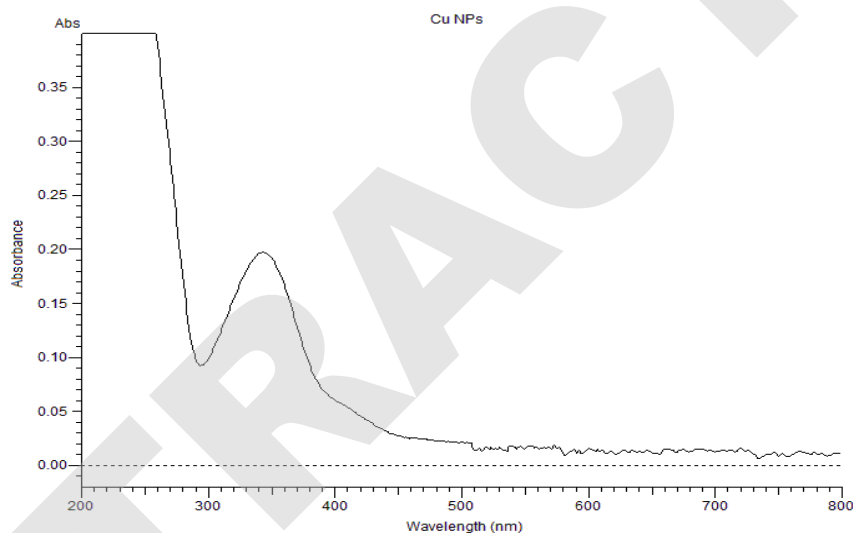

Figure 2. UV-visible absorption spectra of copper oxide nanoparticles

FT-IR analysis of synthesized nanoparticles:

The FT-IR analysis of the copper nanoparticles in the media of the aqueous root extract of *S swietenioides* was conducted in order to identify the bioactive functional groups in the root extract that are responsible for the reduction of metallic copper to the copper oxide nanoparticles. The FT-IR spectrum is given in Figure 3 and the functional groups that were identified by the FT-IR are given in Table 1.

T a b l e 1

Bioactive functional groups identified by the FT-IR spectrum

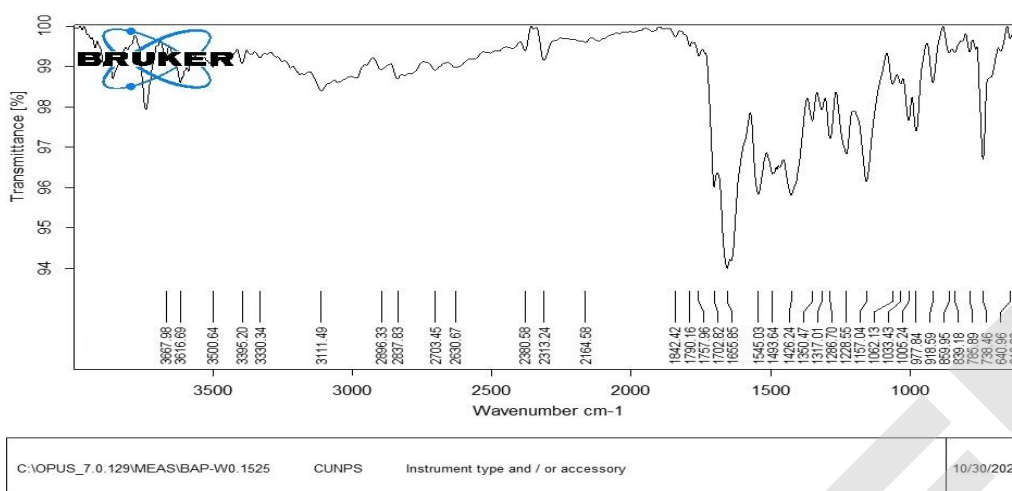| S No	Absorption, cm^{-1}	Functional group
1	3667 & 3616	O-H bond in free and intermolecular bonded alcohols
2	3500	N-H bond in primary amines
3	3395	O-H bond in carboxylic acid
4	3330	N-H bond in aliphatic primary amines
5	1655	C-H bond in aromatic compounds
6	1317	C-O bond in aromatic esters

Figure 3. FT-IR spectrum of copper oxide nanoparticles synthesized using aqueous root extract of *S. swietenioides*

The functional groups determined by the FT-IR analysis of copper oxide nanoparticles were in correlation with the phytochemical solvent extracts of *S swietenioides* leaves. Hence the results confirm the involvement of the plant based biomolecules in the formed nanoparticles.

SEM analysis:

The SEM analysis was performed to determine the size and shape of the copper oxide nanoparticles synthesized using aqueous root extract of *S swietenioides*. The SEM analysis of the copper nanoparticles in the media of the aqueous root extract of *S swietenioides* gives the information about their shape and the size. The FE-SEM analysis was conducted to determine the morphology of Cu NPs. Analysis results are given in Figure 4. The particles were observed to be aggregates with spherical shape and some of them were undefined shape nanoparticles.
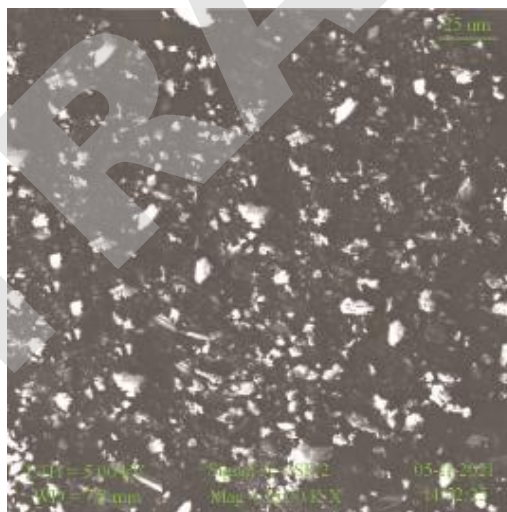

Figure 4. SEM micrograph of the copper nanoparticles in the media of the aqueous root extract of *S swietenioides*

TEM analysis:

TEM is the perfect analytical tool for the chemical and structural characterization of the nano-scale materials. Diffraction, imaging and micro analytical information was obtained from the TEM analysis. The combination of these results describes the behaviour of the nano-sized and nanostructured materials. Thus, TEM analysis of the copper oxide nanoparticles synthesized using aqueous leaf and root extract of *S swietenioides* was carried out.

The TEM analysis of the copper nanoparticles in the media of the aqueous root extract of *S swietenioides* confirms the synthesized nanoparticles were spherical shape. The surface of the individual particle was also studied and it was confirmed the surface of the nanoparticles is smooth. The average parti-

cle size was observed to be 75 nm. The size of the nanoparticles was distributed broadly in the range of 20-95 nm. The result achieved in the TEM analysis was in correlation with the results reported for the same sample in SEM. The TEM micrograph observed for the synthesized copper oxide nanoparticles is given in Figure 5
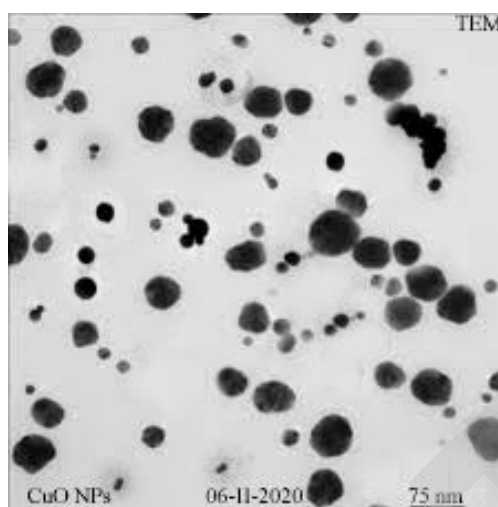

Figure 5. TEM micrograph of the the copper nanoparticles in the media of the aqueous root extract of S swietenioides

XRD analysis:

The lattice phase, crystalline structure, crystalline particle size and crystal lattice parameters of the synthesized nanoparticles were determined by the XRD analysis. Scherrer equation was used for the calculation of the lattice parameters of nanoparticles. The XRD analysis of the copper oxide nanoparticles synthesized using aqueous root extract of *S swietenioides* was carried out.

The XRD spectra of the copper oxide nanoparticles synthesized using aqueous root extract of *S swietenioides* shows the 2θ characteristic peaks corresponds to planes as same as the crystal lattice structure. The peaks identified at 2θ value of 16.38°, 32.15°, 39.81°, 49.87° and 53.20°, which corresponds to (110), (111), (220), (800) and (713) planes of the crystal lattice. Identified peaks and their corresponding planes confirm that the nanoparticles are in monoclinic configuration and their identified planes are in good correlation with the JCPDS standard card number 89-5899. The Scherrer formula (D = 0.9 λ/β cos θ, where β = full width at half maximum at the θ angle and λ = wavelength) was used in calculation of the average crystalline size of the CuNPs and obtained results were at 32±4 nm on the (111) plane. The results achieved in the XRD analysis for the copper oxide nanoparticles synthesized in the study were in good correlation with the results achieved for the same sample in SEM and TEM analysis. The XRD spectra of the copper oxide nanoparticles synthesized in the study is given in Figure 6.
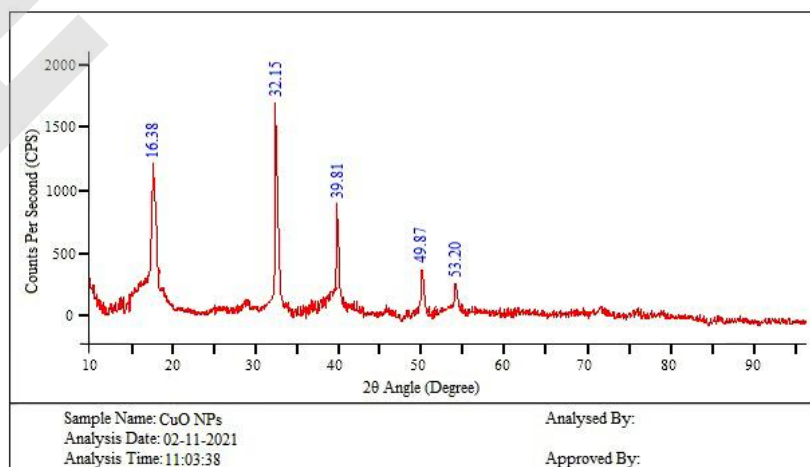

Figure 6. XRD spectrum of the copper nanoparticles in the media of the aqueous root extract of S *swietenioides*

Results and Discussion

Photo catalytic Reduction of Sudan Red (III) Dye Using Copper Oxide Nanoparticles:

The reduction study was performed at various strengths of nano-catalyst and at optimized 10 ppm concentration of Sudan red dye. The result confirms that dose dependent catalytic activity was observed and the reduction activity was increased with the growth in dose of the nano-catalyst. The reduction efficiency was also observed to be increasing with increase in contact time. The reduction efficiency was observed to be high in the initial time of the study and maximum reduction was completed within 45 min of time. The % of reduction at the contact time of 45 min was observed to be 61.23±0.060, 54.28±0.153, 38.13±0.028 and 20.50±0.036 % respectively at nano-catalyst dose of 1.0, 0.75, 0.50 and 0.25 g/L. The reduction time was increased up to 2 h and at the longest studied time the % of reduction was observed to be 84.22±0.051, 79.83±0.062, 54.54±0.576 and 44.44±0.071 respectively at nano-catalyst dose of 1.0, 0.75, 0.50 and 0.25 g/L. Table 2 shows the reduction study of sudan red at various strengths of *S swietenioides* mediated copper oxide nanoparticles and its comparison graph is shown in Figure 7. Comparative UV-visible absorption spectra before and after treatment of Sudan red solution with nanoparticles are presented in Figure 8.

T a b l e   2

Reduction study of Sudan red at various strengths of *S swietenioides* mediated copper oxide nanoparticles

S No	Time in min	% of Sudan red reduction at nano-catalyst strength of			
		0.25 g/L	0.50 g/L	0.75 g/L	1.0 g/L
1	15	17.19±0.060	18.26±0.042	26.86±0.061	29.52±0.071
2	30	21.44±0.031	27.45±0.020	43.09±0.053	54.23±0.067
3	45	39.32±0.065	42.65±0.029	59.64±0.059	69.71±0.025
4	60	42.10±0.042	48.26±0.035	76.19±0.053	81.11±0.044
5	75	43.23±0.038	53.63±0.026	76.90±0.042	82.28±0.075
6	90	43.96±0.070	54.24±0.042	78.49±0.074	82.72±0.040
7	105	44.14±0.062	54.95±0.025	79.18±0.057	83.10±0.075
8	120	44.44±0.071	54.54±0.576	79.83±0.062	84.22±0.051
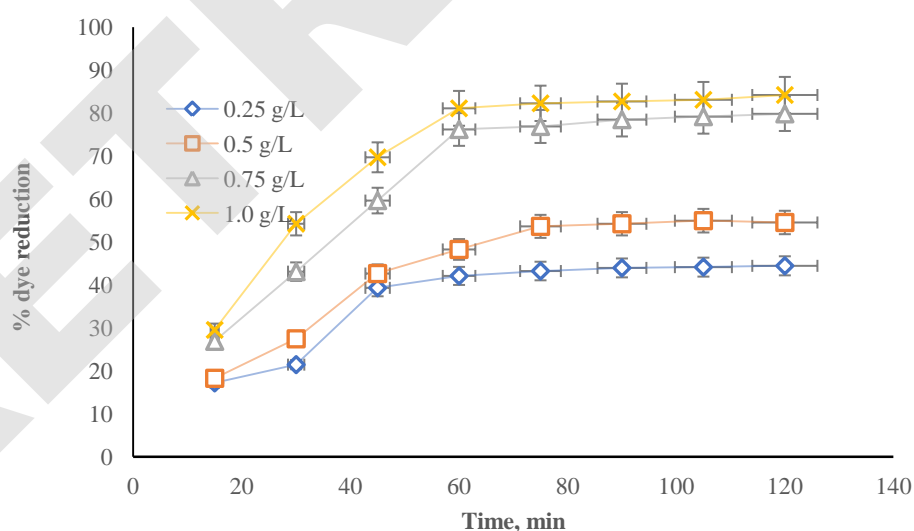
Figure 7. Comparative reduction study results of Sudan red at various strengths
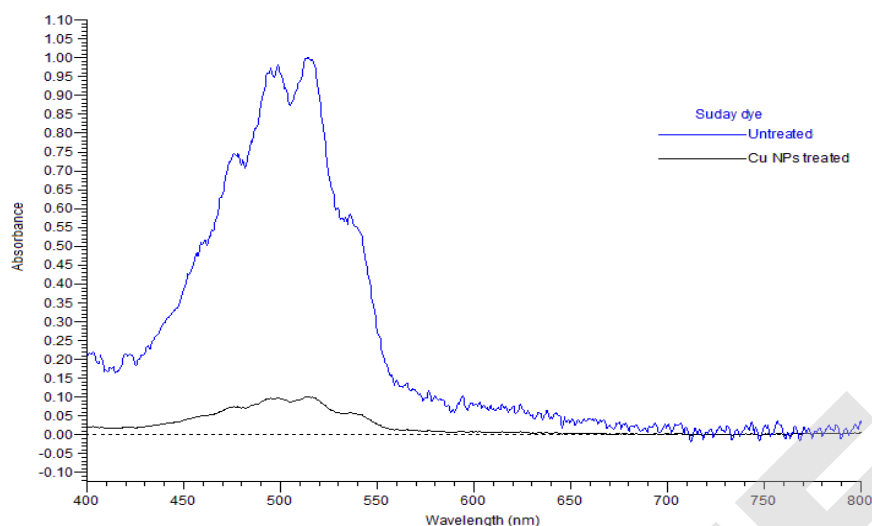of *S swietenioides* mediated copper oxide nanoparticles

Figure 8. Comparative UV-visible absorption spectra before and after treatment
of Sudan red solution with nanoparticles

The rate constant of the catalytic degradation of Sudan red using the synthesized copper oxide nanoparticles was calculated by plotting the graph with the time of reduction study in minutes on *x-axis* and $\ln(A_0/A_t)$ on the *y*-axis. The results confirm that the degradation of Sudan red using copper oxide nanoparticles follows the pseudo first order reaction mechanism for all the doses of nano-catalyst studied. The rate constant (*k*) of the studied strengths of nanoparticles was calculated and the *k* was obtained as 1.37×10^{-2}, 1.27×10^{-2}, 5.85×10^{-3} and 3.77×10^{-3} for the reduction using the nanoparticles at 1.0, 0.75, 0.5 and 0.25 g/L strength respectively. The degradation time profile of treatment of Sudan red solution with copper oxide nanoparticles is given in Figure 9.
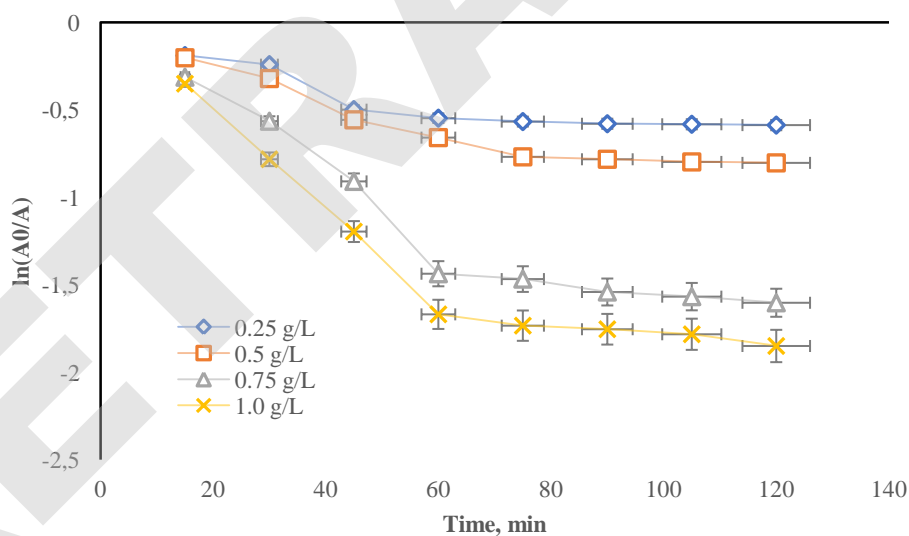

Figure 9. Photo degradation time profile of A_t/A_0 for sudan red dye

Photo Catalytic Reduction of Azure A Dye Using Copper Oxide Nanoparticles:

The reduction study was performed at various strengths of nano-catalyst and at optimized 50 ppm concentration of Azure A dye. The result confirms that dose dependent catalytic activity was observed and the reduction activity was raised with an increase in dose of the nano-catalyst [18]. The reduction efficiency was also observed to be growing with an increase in contact time. The reduction efficiency was observed to be high in the initial time of the study and maximum reduction was completed within 45 min of time. The % of reduction at the contact of 45 min was observed to be 64.00 ± 0.566, 46.71 ± 0.020, 34.24 ± 0.026 and

29.32±0.050 % respectively at nano-catalyst dose of 1.0, 0.75, 0.50 and 0.25 g/L. The reduction time was increased up to 2 h and at the longest studied time the % of reduction was observed to be 81.62±0.663, 80.65±0.040, 60.54±0.032 and 39.70±0.044 respectively at nano-catalyst dose of 1.0, 0.75, 0.50 and 0.25 g/L. Table 3 shows the reduction study of azure A at various strengths of *S swietenioides* mediated copper oxide nanoparticles and its comparison graph is shown in Figure 10. Comparative UV-visible absorption spectra before and after treatment of Azure A solution with nanoparticles are presented in Figure 11.

T a b l e 3

Reduction study of Azure A at various strengths of *S swietenioides* mediated copper oxide nanoparticles

| S No	Time in min	% of Azure A reduction at nano-catalyst strength of			
		0.25 g/L	0.50 g/L	0.75 g/L	1.0 g/L
1	15	8.24±0.031	9.67±0.060	17.35±0.035	38.40±4.505
2	30	15.35±0.049	21.62±0.036	35.13±0.057	49.76±0.451
3	45	29.32±0.050	34.24±0.026	46.71±0.020	64.00±0.566
4	60	36.81±0.040	41.11±0.025	69.43±0.020	73.38±0.606
5	75	37.12±0.031	58.71±0.084	78.35±0.023	79.36±0.636
6	90	38.18±0.040	59.24±0.042	79.67±0.060	80.08±0.678
7	105	39.15±0.072	59.86±0.050	80.12±0.030	80.93±0.655
8	120	39.70±0.044	60.54±0.032	80.65±0.040	81.62±0.663
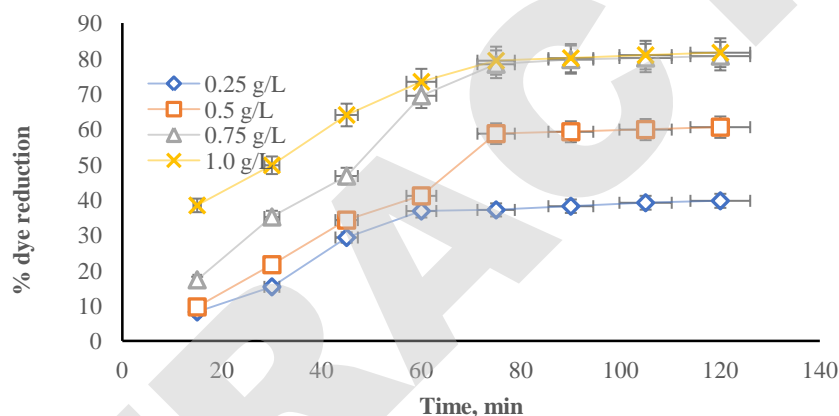
Figure 10. Comparative reduction study results of Azure A at various strengths of *S swietenioides* mediated copper oxide nanoparticles
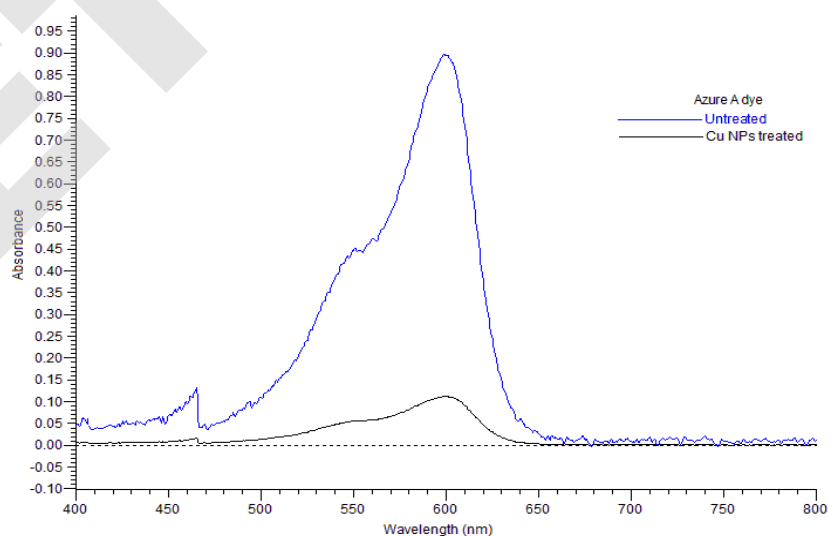

Figure 11. Comparative UV-visible absorption spectra before and after treatment of Azure A solution with nanoparticles

The rate constant of the catalytic degradation of Sudan red using the synthesized copper oxide nanoparticles was calculated by plotting the graph with the time of reduction study in minutes on *x-axis* and $\ln(A_0/A_t)$ on the *y*-axis. The results confirm that the degradation of Sudan red using copper oxide nanoparticles follows the pseudo first order reaction mechanism for all the doses of nano-catalyst studied. The rate constant (k) of the studied strengths of nanoparticles was calculated and the k was obtained as 1.28×10^{-2}, 1.53×10^{-2}, 8.69×10^{-3} and 3.96×10^{-3} for the reduction using the nanoparticles at 1.0, 0.75, 0.5 and 0.25 g/L strength respectively. The degradation time profile of treatment of Azure A solution with copper oxide nanoparticles is given in Figure 12.
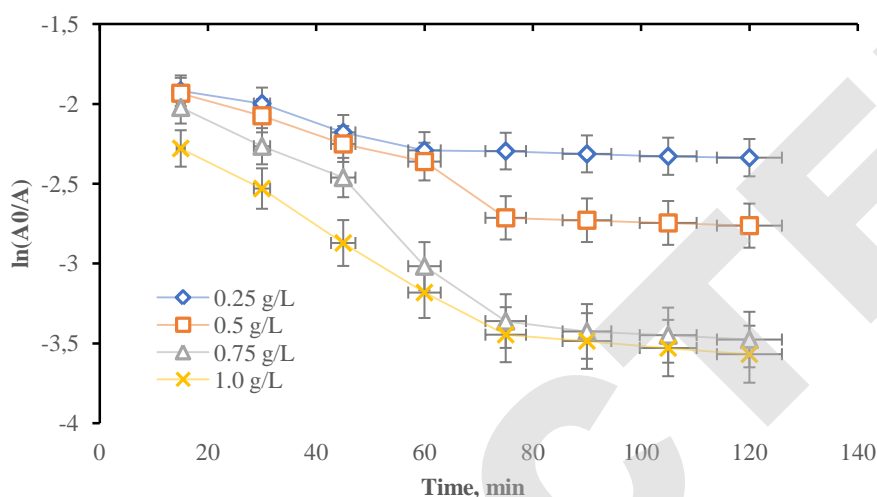

Figure 12. Photo degradation time profile of A_t/A_0 for azure A dye

Photo catalytic Reduction of Lead Metal Using Copper Oxide Nanoparticles:

The reduction study was performed at various strengths of nano-catalyst and at optimized 50 µg/mL concentration of lead metal. The result confirms that dose dependent catalytic activity was observed and the reduction activity was raised with an increase in dose of the nano-catalyst [19]. The reduction efficiency was also observed to be increasing with an increase in contact time. More than 50 % of the reduction was observed within the time of 45 min at a nano catalyst-dose of 0.75 and 1.0 g/L and the observed degradation was at 54.28±0.153 and 61.23±0.060 % respectively. The reduction time was increased up to 2 h and at the longest studied time the % of reduction was observed to be 88.94±0.026, 81.02±0.127, 66.15±0.023 and 39.60±0.048 % respectively at nano-catalyst dose of 1.0, 0.75, 0.50 and 0.25 g/L. Table 4 shows the reduction study of lead metal at various strengths of *S swietenioides* aqueous root extracts mediated copper oxide nanoparticles and its comparison graph is shown in Figure 13. The comparative UV-vis absorption spectra obtained for before and after treatment of lead — dithizone complex solution with nanoparticles are given in Figure 14.

Table 4

Reduction study of lead metal at various strengths of *S swietenioides* mediated copper oxide nanoparticles

| S No	Time in min	% of lead reduction at Nano catalyst strength of			
		0.25 g/L	0.50 g/L	0.75 g/L	1.0 g/L
1	15	8.04±0.016	13.46±0.055	20.77±0.062	24.48±0.076
2	30	13.73±0.026	27.22±0.041	34.82±0.039	39.18±0.540
3	45	20.50±0.036	38.13±0.028	54.28±0.153	61.23±0.060
4	60	29.91±0.029	51.59±0.070	73.11±0.088	82.45±0.059
5	75	36.24±0.039	64.98±0.055	78.57±0.039	87.60±0.061
6	90	38.06±0.023	65.35±0.032	79.62±0.129	85.86±4.027
7	105	39.07±0.024	65.50±0.044	80.20±0.098	88.72±0.046
8	120	39.60±0.048	66.15±0.023	81.02±0.127	88.94±0.026
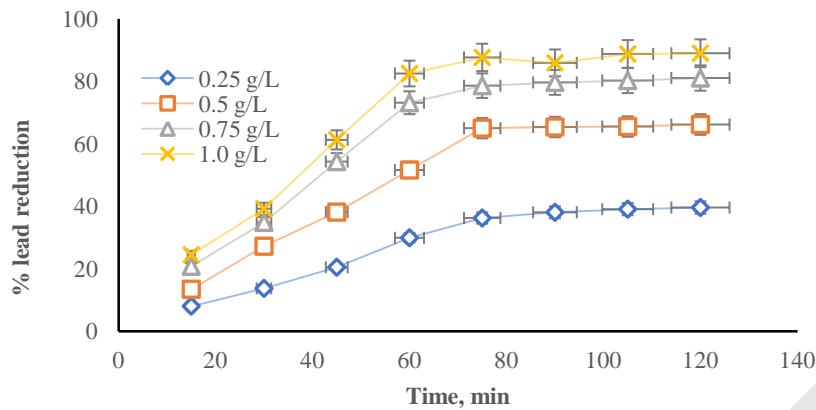
Figure 13. Comparative reduction study results of lead metal at various strengths of *S swietenioides* mediated copper oxide nanoparticle
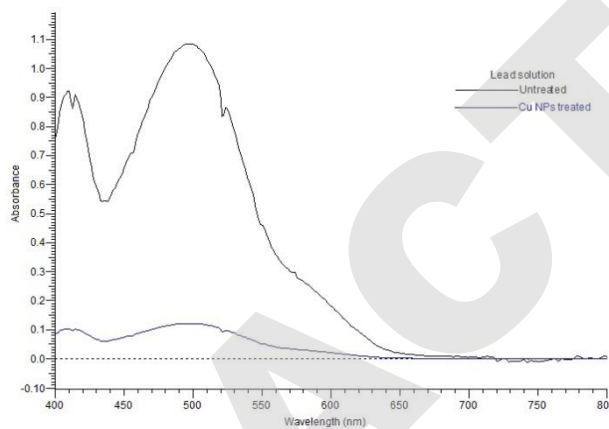

Figure 14. Comparative UV visible absorption spectra before and after treatment of lead – dithizone complex solution with nanoparticles

The rate constant of the catalytic degradation of lead metal using the synthesized copper oxide nanoparticles was calculated by plotting the graph with the time of reduction study in minutes on *x-axis* and $\ln(A_0/A_t)$ on the *y*-axis. The results confirm that the degradation of Sudan red using copper oxide nanoparticles follows the pseudo first order reaction mechanism for all the doses of nano-catalyst studied. The rate constant (k) of the studied strengths of nanoparticles was calculated and the k was obtained as 2.04×10^{-2}, 1.47×10^{-2}, 9.80×10^{-3} and 4.38×10^{-3} for the reduction using the nanoparticles at 1.0, 0.75, 0.5 and 0.25 g/L strength respectively. The degradation time profile of treatment of lead metal with copper oxide nanoparticles is given in Figure 15.
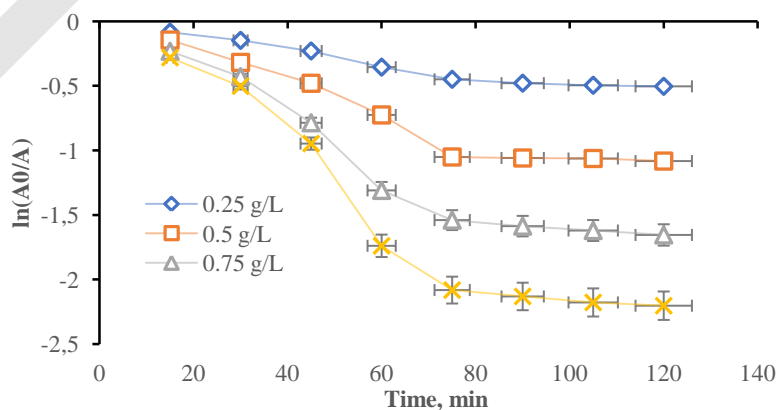

Figure 15. Photo degradation time profile of A_t/A_0 for lead metal

Conclusions

To sum up, it can be concluded that the study confirms the green synthesis of copper oxide nanoparticles using aqueous root extract of *Schrebera swietenioides* Roxb. The synthesized nanoparticles have been characterized and it was proved the particles were nano-sized and contained high metal percentage. The obtained nanoparticles were effective in the photo catalytic degradation of various carcinogenic pollutant dyes and metals and they can be used in the photo catalytic reduction of various pollutant dyes and metals, such as Sudan red (III), Azure A and lead metal) and were proven to be effective. The synthesized copper nanoparticles were found to be stable up to five cycles of the photo catalytic reduction process in all the dyes and metal in the study.

Acknowledgments

References

1   Shahid, M., Dumat, C., Khalid, S. et al. (2017). Foliar heavy metal uptake, toxicity and detoxification in plants: a comparison of foliar and root metal uptake. *J Hazardous Mater, 325*, 36–58. https://doi.org/10.1016/j.jhazmat.2016.11.063

2   Pal, G., Rai, P., & Pandey, A. (2019). Chapter 1 — Green synthesis of nanoparticles: a greener approach for a cleaner future. In: Shukla AK, Iravani (eds.). *Characterization and applications of nanoparticles SBT-GS micro and nano technologies*, Elsevier, Amsterdam, 1–26. https://doi.org/10.1016/B978-0-08-102579-6.00001-0

3   Gahlawat, G., & Roy, C. A. (2019). A review on the biosynthesis of metal and metal salt nanoparticles by microbes, *RSC Adv, 9*(23), 12944–12967. https://doi.org/10.1039/c8ra10483b

4   Iravani, S. (2011). Green synthesis of metal nanoparticles using plants. *Green Chem, 13*, 2638–2650. http://dx.doi.org/10.1039/c1gc15386b

5   Singh, J., Kumar, V., Kim, K. H., & Rawat M. (2019). Biogenic synthesis of copper oxide nanoparticles using plant extract and its prodigious potential for photocatalytic degradation of dyes. *Environmental research, 177*, 108569. https://doi.org/10.1016/j.envres.2019.108569

6   Ismail, N. A., Shameli, K., Che, J. N. W., Rasit, A. R., Mohamad, S. N. A. & Mohamed, I. E. D. (2021). Preparation of Copper Nanoparticles by Green Biosynthesis Method: A Short Review. *IOP Conf. Series: Materials Science and Engineering, 1051*, 012084. https://doi.org/10.1088/1757-899X/1051/1/012084

7   Ananda, M. H. C., Buzuayehu, A., Prakash, C. H. & Kumar, S. (2018). A Review on Green Synthesis of Cu and CuO Nanomaterials for Multifunctional Applications, *Mat Sci Res India, 15*(3), 279–295. http://dx.doi.org/10.13005/msri/150311

8   Elsy, R. L. V., Hortensia, O. O., Gregorio, C. P., Karim, A. R., Marcelino, C. F., Adalberto, B. M. & Antonio, J. M. (2018). Application of Copper Nanoparticles Increases the Fruit Quality and the Content of Bioactive Compounds in Tomatoes. *Appl Sci, 8*, 1020. https://doi.org/10.3390/app8071020

9   Kandasamy, S., Anbazhagan, S., Arokia, V. A. M., Hu, X., & Myeong, H. W. (2020). Physical and bioactivities of biopolymeric films incorporated with cellulose, sodium alginate and copper oxide nanoparticles for food packaging application. *International Journal of Biological Macromolecules, 153*, 207–214. https://doi.org/10.1016/j.ijbiomac.2020.02.250

10   Ghosh, M. K., Sahu, S., Gupta, I. & Ghorai, T. K. (2020). Green synthesis of copper nanoparticles from an extract of Jatropha curcas leaves: characterization, optical properties, CT-DNA binding and photocatalytic activity. *RSC Adv, 10*(37), 22027–22035. https://doi.org/10.1039/d0ra03186k

11   Suresh, C. M., Anita, D., Chanda, K. G., & Rohini, T. (2020). Green synthesis of copper nanoparticles using Celastrus paniculatus Willd. leaf extract and their photocatalytic and antifungal properties. *Biotechnology Reports, 27*, 00518. https://doi.org/10.1016/j.btre.2020.e00518

12   Peddi, P., Rao, P., Rani, N. U., & Lakshmi Tulasi, S. (2021). Green synthesis, characterization, antioxidant, antibacterial, and photocatalytic activity of Suaeda maritima (L.) Dumort aqueous extract-mediated copper oxide nanoparticles. *J Genet Eng Biotechnol., 19*, 1–11. https://doi.org/10.1186/s43141-021-00229-9

13   Siddique, M., Fayaz, N., & Saeed, M. (2021). Synthesis, characterization, photocatalytic activity and gas sensing properties of zinc doped manganese oxide nanoparticles. *Physica B: Condensed Matter, 602*, 412504. https://doi.org/10.1016/j.physb.2020.412504

14   Khan, I., Saeed, K., & Khan, I. (2019). Nanoparticles: Properties, applications and toxicities. *Arabian Journal of Chemistry, 12*(7), 908–931. https://doi.org/10.1016/j.arabjc.2017.05.011

15   Kulkarni, N., & Muddapur, U. (2014). Biosynthesis of metal nanoparticles: a review. *J. Nanotechnol*, 510246. https://doi.org/10.1007/978-3-642-18312-6_3

16   Mohammod, A., Leong, M. K., & Wong, H. L. (2017). Green synthesis of copper oxide (CuO) nanoparticles using banana peel extract and their photocatalytic activities. *AIP Conference Proceedings, 1828*, 020016. https://doi.org/10.1063/1.4979387

17 Shraddha, P., Sridevi, H., Thivaharan, V., Ramesh, V. & Raja, S. (2019). Photocatalytic zinc oxide nanoparticles synthesis using Peltophorum pterocarpum leaf extract and their characterization. *Optik, 185*, 248–255. https://doi.org/10.1016/j.ijleo.2019.03.101

18 Ozge, C., Emre, N., Umut, K., Sirous, K. A., Cleva, W. O. & Havva, Y. A. (2020). Synthesis of stable gold nanoparticles using linear polyethyleneimines and catalysis of both anionic and cationic azo dye degradation. *Mater. Adv, 1*, 2407–2417. https://doi.org/10.1039/d0ma00404a

19 Khoso, W. A.., Haleem, N., Baig, M. A. et al. (2021). Synthesis, characterization and heavy metal removal efficiency of nickel ferrite nanoparticles (NFN's). Sci Rep, 11, 3790–3799. https://doi.org/10.1038/s41598-021-83363-1

Information about authors*

Tulasi, Lakshmi S. (*corresponding author*) — Assistant Professor, Department of Freshman Engineering, PVP Siddhartha Institute of Technology, Kanuru-52007, Vijayawada, Andhra Pradesh, India; e-mail: tulasi13111986@gmail.com; https://orcid.org/0000-0001-6130-7215;

Sumalatha, P. — Assistant Professor, BS&H Department, Seshadri Rao Gudlavalleru Engineering college, Gudlavalleru. Andhra Pradesh, India; e-mail: sumasobhan@gmail.com; https://orcid.org/0000-0001-7230-4976

Rani, Nannapaneni Usha — Assistant Professor Dept. of Freshman Engineering, PVP Siddhartha Institute of Technology, Kanuru, 52007 Vijayawada, Andhra Pradesh, India. e-mail: nannapaneniusharani73@gmail.com;

Peddi, Pavani — Assistant Professor, Department of Freshman Engineering, PVP Siddhartha Institute of Technology, Kanuru-520007 Vijayawada, Andhra Pradesh, India, e-mail: pavanipeddi7@gmail.com; https://orcid.org/0000-0003-0712-8907

_____

*The author's name is presented in the order: *Last Name, First and Middle Names*